Moment tensor inversion for the source location and mechanism of long period (LP) seismic events from 2009 at Turrialba volcano, Costa Rica

Thomas S. Eyre [a], Christopher J. Bean [a], Louis De Barros [a, 1], Gareth S. O'Brien [a, 2], Francesca Martini [a, 2], Ivan Lokmer [a], Mauricio M. Mora [b], Javier F. Pacheco [c] and Gerardo J. Soto [d]

[a] *Seismology and Computational Rock Physics Laboratory, School of Geological Sciences, University College Dublin, Belfield, Dublin 4, Ireland. tom.eyre@ucd.ie, Chris.Bean@ucd.ie, ivan.lokmer@ucd.ie*

[b] *Escuela Centroamericana de Geología, Universidad de Costa Rica, San José, Costa Rica. mauricio.mora@ucr.ac.cr*

[c] *Ovsicori-UNA, Universidad Nacional, Heredia, Costa Rica. jpacheco@una.ac.cr*

[d] *Instituto Costarricense de Electricidad (ICE), San José, Costa Rica. katomirodriguez@yahoo.com*

[1] *Now at: Géoazur, Université de Nice Sophia-Antipolis, CNRS, Observatoire de la Côte d'Azur, 250 rue Albert Einstein, Sophia-Antipolis, 06560 Valbonne, France. debarros@geoazur.unice.fr*

[2] *Now at: Tullow Oil Ltd, Dublin, Ireland. Gareth.OBrien@tullowoil.com, Francesca.Martini@tullowoil.com*

Corresponding Author

Thomas S. Eyre

Seismology and Computational Rock Physics Laboratory,

School of Geological Sciences,

University College Dublin,

Belfield,

Dublin 4,

Ireland

Phone: +353 1 716 2079

Fax: +353 1 283 7733

Email: tom.eyre@ucd.ie

Abstract

Long-period (LP) seismic events were recorded during the temporary installation of a broadband seismic network of 13 stations from March to September 2009 on Turrialba volcano, Costa Rica. Over 6000 LPs were extracted using a modified STA/LTA method and a family consisting of 435 similar LP events has been identified. For the first time at Turrialba volcano, full-waveform moment tensor inversion is performed to jointly determine the location and source mechanism of the events. The LPs in the family are likely to be caused by crack mechanisms dipping towards the southwest at angles of approximately 10 to 20 degrees, located at shallow depths (< 800 m) below the active Southwest and Central craters. As the locations are so shallow, the most probable causes of crack mechanisms are hydrothermal fluids resonating within or "pulsing" through a crack. The waveforms observed at the summit stations suggest a "pulsing" mechanism, but source resonance with a high degree of damping is also possible.

Keywords: *volcano; seismicity; long period (LP) events; moment tensor inversion; Turrialba volcano*

1. Introduction

Turrialba volcano is a large (3340m a.s.l.) basaltic-andesitic stratovolcano located at the eastern edge of the Cordillera Volcánica Central, Costa Rica, Central America, 35km ENE of the capital San José (figure 1a). This close proximity to San José makes monitoring the volcano extremely important, as a large eruption has the potential to affect 1.5 million people (Soto et al., 2010). The most recent major eruptive event occurred between 1864 and 1866 and comprised phreatic, magmatic and phreatomagmatic episodes, including the generation of pyroclastic flows and surges (Reagan et al., 2006; Soto, 1988).

The volcano summit is characterised by three main craters (named Northeast, Central and Southwest due to their geographical positions) in a linear configuration, reflecting the movement of the active

volcanic centre from Northeast to Southwest (Martini et al., 2010; Soto, 1988). Fumarolic gas discharges have been continuously present since the end of the last eruption (Campion et al., 2012; Soto, 1988; Soto and Mora, 2013; Tassi et al., 2004; Vaselli et al., 2010). However since 1996, the volcano has been showing signs of increased fumarolic activity as well as increased levels of seismicity. This culminated in phreatic explosions beginning on 4th January 2010 (Barquero and Rojas, 2011; Martini et al., 2010; Soto and Mora, 2013), opening a vent with dimensions of approximately 65m by 20m on the southwest inner wall of the Southwest crater.

Long period (LP) seismic events have previously been observed at Turrialba volcano (Martini et al., 2010; Soto and Mora, 2013), and their numbers have increased since 1996. This type of event occurs at volcanoes across the world, often increasing in number before a volcanic eruption (Chouet, 1996; Varley et al., 2010). For the past few decades, efforts have been made in order to understand the sources of LP events. Experimentation, modelling, direct observations and technological advancements have been applied at active volcanoes across the world in order to come up with plausible models for LP events. Many models attribute them to fluid processes in order to explain their lack of energy at frequencies above 5 Hz, with the principle model proposing that they are caused by resonance of a fluid-filled cavity (Chouet, 1988; Jousset et al., 2004; Neuberg et al., 2006). The resonance produces slow waves that travel along the interface of the cavity (often called crack waves) at velocities lower than the acoustic velocity in the fluid, facilitating the generation of low frequency events even from relatively small cavities (Chouet, 1986; Ferrazzini and Aki, 1987). The excitation mechanism for the resonance remains unclear, but could be related to pressure fluctuations within the fluid caused by fluid motion (Gilbert and Lane, 2008; Neuberg et al., 2006; Ohminato et al., 1998; Rust et al., 2008). The fluid within the cavity could be hydrothermal (Cusano et al., 2008; Kumagai et al., 2005), gas (Lokmer et al., 2007) or magma (Neuberg et al., 2006).

Full-waveform moment tensor inversion of LP events has been carried out at several volcanoes across the world (see review from Chouet and Matoza (2013)), including Kilauea, Hawaii (Kumagai et al., 2005), Mt Etna, Sicily (De Barros et al., 2011; Lokmer et al., 2007), Kusatsu-Shirane, Japan (Kumagai et al., 2002) and Campi Flegrei, Italy (Cusano et al., 2008). The source mechanisms are

usually constrained as crack mechanisms, which (using the resonance model for source generation) are often interpreted as fluid-filled cracks that are excited into resonance (Cusano et al., 2008; Kumagai et al., 2002; Kumagai et al., 2005). These mechanisms are often accompanied by single forces, which could be caused in volcanic environments by transfer of mass within the volcano (Chouet, 2003; Takei and Kumazawa, 1994), drag forces (Ohminato et al., 1998), or by a volcanic jet during an explosion (Jolly et al., 2010). However, single forces recovered during moment tensor inversion are often artefacts caused by mismodelling of the velocity structure during the inversion (De Barros et al., 2011).

No studies have previously been carried out to investigate the source mechanism of LP events on Turrialba volcano, making this the first in-depth study. This study is therefore important as a better comprehension of LP events at Turrialba volcano may improve the understanding of the present stage of activity within a potentially dangerous volcano that appears to be "reawakening". Turrialba volcano is also an ideal candidate for moment tensor inversion of LP events due to the relative ease of access to the summit of the volcano in comparison to many other active volcanoes; the summit region is large and relatively flat, allowing for the dense deployment of seismometers close to the active craters, which reduces the likelihood of erroneous solutions (Bean et al., 2008; Kumagai et al., 2010).

The aim of this study is to accurately locate and resolve the source mechanisms of LP events at Turrialba volcano, using experience gained from previous studies, e.g. Davi et al. (2010); Lokmer et al. (2007). The results are interpreted in terms of the processes within Turrialba volcano and compared to those for other volcanoes globally.

2. Data

A seismic field experiment was undertaken between 19th March and 8th September 2009 at Turrialba volcano. During the experiment, 13 stand-alone broadband seismometers were deployed (figure 1b); however only 10 were functioning for the majority of the time. CIMA, CIM2 and CEN1 are Guralp 3ESPDC 60 second instruments and the remaining stations are Guralp 6TD 30 second instruments. The sampling rate was 100 samples/sec. The network was designed to have a high density

distribution of stations across the summit and flanks of the volcano, which has been suggested by Bean et al. (2008) and De Barros et al. (2011) to be necessary for accurate source inversion: this was difficult to achieve in some areas on the northern flank of the volcano which is inaccessible.

LP events are extracted from the data using short time average over long time average (STA/LTA) analysis within a frequency band of 0.5 to 4.0 Hz and a threshold of 6. However, this criterion also picks out other volcano-seismic events including volcano-tectonic (VT) events, which are not used in this study. An example of an LP event and an "unwanted" seismic event (VT) is shown in figure 2, with the LP at ~ 40 s and the VT event at ~ 70 s. In order to filter out the unwanted events, the STA/LTA analysis is also carried out separately for a higher frequency band (6.0 to 10.0 Hz). VT events would have a high (above threshold) STA/LTA value for both the low frequency and the high frequency bands (for example, the event on the right of figure 2 has an STA/LTA value of 17.6 for the low frequency band and 13.7 for the high frequency band), whereas LP events would have a high STA/LTA value for low frequencies only (the LP in figure 2 has a value of 39.8 for the low frequency band and 7.2 for the high frequency band). Therefore, events are only picked if they have a STA/LTA response more than 4 times larger in the low frequency band than in the higher frequency band. For the events in figure 2, this low-to-high frequency STA/LTA ratio is equal to 5.5 for the LP event (picked) and 1.3 for the VT event (rejected). Using this technique, over 6000 LP events are picked at the summit seismic station CIMA for the duration of the experiment. This station is used as it is closest to the active craters and is also one of the 60 second instruments. An example of an LP event recorded during the experiment is shown for the Z component at all stations in figure 3a.

The events are grouped into families of similar events using a cross-correlation method. The LPs are filtered between 0.3 and 1.3 Hz as most LPs recorded at Turrialba volcano have a main peak in this range of frequencies (figure 3b). They are cut 4 s before the minimum and 6 s afterwards, giving a 10 s trace to correlate. Each event is systematically correlated with all of the other events: subsequently, cluster analysis groups the events into families, where all correlation coefficients for events within a family are greater than a threshold of 0.8 (closed cluster). Using this technique, five separate families of events are extracted. The mean amplitude stacks of these families are shown in figure 4a, along

with the number of events in each family. It can be seen that while each family appears to have slightly different waveforms, the differences between each stack are actually quite small. When the stacks are correlated with each other, they all correlate above the correlation coefficient threshold of 0.8. As stacking is a way of increasing the signal-to-noise ratio, and these stacks now correlate above the threshold, the five families are grouped together into one large family of 435 events, the mean amplitude stack of which is shown in figure 4b. However, the small differences in waveforms between the stacks of the original five families suggest that very small changes in source location and/or mechanism may occur between events.

The events show a pulse-like waveform in the frequency band used for the correlation (0.3 to 1.3 Hz). The correlated LPs have high amplitude (of the order of 10^{-5} m/s) and the first polarity is always positive.

It is noted that although a large family has been formed, this family represents only a small number of the total events recorded (< 8 %), leaving thousands of events that are not well correlated. Figure 5 shows the temporal distribution of LP events from the family (black), as well as the total number of LP events (red). Note that the apparent gap in LP activity during July is caused by a problem with station CIMA. It is interesting to note that the numbers of events that cluster into the family proportionally decrease with time.

3. 3D Full-Waveform Moment Tensor Inversion

The source mechanism for the LP events is determined by using full waveform moment tensor inversion (Chouet et al., 2003; De Barros et al., 2011; Kumagai et al., 2002; Ohminato et al., 1998). The method used here is described in detail in Davi et al. (2010). The *n*th component of the displacement *u*, recorded at position **x** and time *t*, can be written as:

$$u_n(\mathbf{x},t) = M_{pq}(t) * G_{np,q}(\mathbf{x},t) + F_p(t) * G_{np}(\mathbf{x},t), \qquad n, p, q = x, y, z \qquad (1)$$

where M_{pq} is the force couple in the direction *pq*, F_p is the single force acting in the direction *p*, and G_{np} and $G_{np,q}$ are the *n*th components of the Green's functions and their spatial derivatives,

respectively, generated by the single force F_p and the moment M_{pq}, respectively. Green's functions are the displacement responses recorded at the receivers when an impulse force function is applied at the source position in an elastic Earth (the medium response). The asterisks indicate convolution and the summation convention applies.

A 3D Elastic Lattice Method (ELM) is used to calculate the Green's functions by simulating full wavefield seismic wave propagation (O'Brien and Bean, 2004). The models include topography which has been shown to be necessary for an accurate inversion in volcanic settings (Bean et al., 2008; Ripperger et al., 2003). Good knowledge of the seismic velocity structure, especially of near-surface low velocity layers that are often present on volcanoes, is also important in order to gain an accurate moment tensor inversion solution (Bean et al., 2008). Unfortunately, no complete velocity models are currently available for Turrialba volcano so a homogeneous model is used. The inaccuracy of the velocity model must be taken into account when interpreting the results. Based on velocities gained from shallow (< 80 m depth) refraction seismology surveys completed on Turrialba volcano in 2009 (Montoya, 2009), the P-wave velocity is assumed to be 3000 m/s, S-wave velocity 1750 m/s and density 2300 kg/m³ for the numerical model used to calculate the Green's functions.

Equation (1) is linear, and in the frequency domain can be written in matrix form:

$$\mathbf{d = Gm} \qquad (2)$$

where **d** is the data matrix, **G** contains the Green's functions, and **m** contains the moment tensor and single forces components. The quality of the inversion results is tested through the evaluation of the misfit between the calculated and the observed data, herein referred to as the residual *R*:

$$R = \frac{\mathbf{d-Gm}^{T}\mathbf{W}\ \mathbf{d-Gm}}{\mathbf{d}^{T}\mathbf{Wd}} \qquad (3)$$

where **W** is a diagonal matrix of weights for the quality of the data.

Inversions are carried out both excluding and including single forces in the solution. De Barros et al. (2011) state that when single forces are included in the moment tensor inversion for a dense network,

the moment tensor component of the solution may be more accurate because the single forces absorb the errors in the velocity models used to estimate the Green's functions. Consequently, the results for the single forces themselves cannot be reliably interpreted. To check the robustness of the solutions the results both including and excluding single forces are examined in this study, although the single forces themselves are not interpreted.

Inversion is carried out for a grid of possible source locations below the volcano summit in order to locate the events through a joint inversion, as has been demonstrated in previous studies (Chouet et al., 2003; Kumagai et al., 2005; Kumagai et al., 2010; Nakano and Kumagai, 2005; Ohminato et al., 1998). As the number of possible source positions is much greater than the number of stations, the Reciprocity Theorem (Aki and Richards, 2002) is used to compute the Green's functions. The most likely location area is defined by the set of smallest residuals described by equation (3).

The moment tensors are then decomposed into their principle components to find the source mechanisms, using the methods of Vasco (1989). This is based on the singular value decomposition of the six time-dependent moment tensor components. This leads to an estimation of a common source-time function and its contribution to each component of the moment tensor, thus giving a source-time history of the source process and its mechanism. The eigenvalues of the scalar moment tensor give the source mechanism and the eigenvectors give the orientation of the principal axes. From this, the solution can be decomposed into the percentage of isotropic, compensated linear vector dipole (CLVD) and double couple source mechanisms (Vavryčuk, 2001), although this is nonunique and sometimes unstable.

4. Results

Results are similar for all events that have been inverted from the family, as expected. Therefore, the results shown in the figures are from the single LP event shown in figure 3. This event is chosen as it has a good signal-to-noise ratio. The peak frequency is approximately 0.65 Hz, and the events are therefore inverted between 0.3 and 1.3 Hz. Only 10 stations are available for the inversion of this event as BABO, CEN1 and GUAY were not functioning at that time (data gaps at stations are a

problem throughout the experiment), but these stations are not in the summit region so have a relatively small contribution to the inversion results. The event used is therefore deemed a good candidate for inversion as many other events have summit station data missing.

4.1 Event Location

Figure 6 shows the results of the gridsearch location method. The results are shown only for the inversion including single forces as results are very similar whether single forces are included or not (this demonstrates the robustness of the solutions).

The gridpoints with the lowest residuals are located below the summit region of Turrialba volcano at shallow depths. The minimum residual is located in UTM grid zone 17P, 196840 m East and 1108840 m North. The depth range is from 0 m to ~ 800 m below the summit; it is impossible to further constrain this due to the lack of an accurate seismic velocity model. The blue volume in the figure shows the region within ~ 5 % of the minimum residual. The possible source area is therefore a large elongated volume from the north-western flank to the south-eastern flank of the volcano, between the active Southwest and Central craters. The radius of this volume is less than 500 m from the minimum residual, giving an error estimate for the location of ~ ± 500 m. Note that several local minima are present, which may lead to erroneous solutions if the network was less dense.

4.2 Source Mechanism

The moment tensor results from the full waveform moment tensor inversion, for the source location with the lowest residual, are shown in figure 7. Normalised waveform fits between the real data and data reconstructed from the moment tensor solution convolved with the Green's functions can be seen in figure 8. The fits are generally good for stations close to the summit of the volcano but poor for the stations further from the summit, which is expected due to the stronger path effect contribution to distant stations. However, the low amplitudes recorded at these stations give implicitly lower weights to these data in the inversion procedure.

The maximum amplitude for M_{zz} is greater than $4x10^{12}$ Nm without forces included in the inversion. When the single forces are included in the inversion they appear to be quite large, ~ 3×10^9 N, but as previously stated these tend to absorb the errors in the inversion and so cannot be taken as evidence that single forces are present (De Barros et al., 2011). The waveforms are pulse-like when the single forces are not included, but when single forces are included the coda of the event is longer. It appears that in this case the moment tensor-only solution is more realistic as the waveform at the summit station CIMA is pulse-like in the same frequency band, which suggests that the source-time function should also be pulse-like. However, except for their pulse-like nature, it is difficult to draw conclusions from the shape of the waveforms due to (i) the uncertainty in the Green's functions calculations regarding the velocity model, and (ii) the limited frequency range of the signals used in the inversion.

The moment tensors have been decomposed into their principle components using the methods of Vavryčuk (2001), Chouet et al. (2003) (figure 7) and Vasco (1989). The results are also listed in tables 1 and 2, for the solutions excluding and including single forces respectively, as well as the results for four other events from the one large family. For all cases, the decomposition produces a long axis eigenvector and two shorter eigenvectors. A tensile crack source produces a $\lambda : \lambda : (\lambda + 2\mu)$ ratio of moment tensor eigenvalues (Aki and Richards, 2002), which is 1 : 1 : 3 for a Poisson's ratio of 0.25 and 1 : 1 : 2 for a Poisson's ratio of 0.35. As the results are within this range, the source mechanism is interpreted as a crack mechanism. The orientations of the longest axes are consistent between events. Excluding single forces, the angle of dip is between 18 ° and 23 °, in a dip direction of between 235 ° to 272 ° anticlockwise from east, i.e. towards the southwest. When single forces are included in the analysis, the dip angle is slightly lower, between 12 ° and 17 °, with a dip direction again towards the southwest, although with a slightly different angle of 204 ° to 215 °. These results imply similar mechanisms for all of the 5 LP events, i.e. crack mechanisms orientated with shallow (approximately 10 ° to 20 °) dip angles towards the southwest. Solutions are similar for source locations within 500 m of the locations used, in all directions, always giving shallowly dipping crack mechanisms, demonstrating that the solution is stable.

In order to confirm that the results can be interpreted as a crack mechanism shallowly dipping to the southwest, constrained inversions are also implemented. During the inversion, the mechanism is constrained to (1) an isotropic source, and (2) a crack with a gridsearch on its dip and azimuth (for details, see Lokmer et al. (2007), De Barros et al. (2011)). These tests also find a crack mechanism to be the best fit solution, with orientations that are very similar to the unconstrained inversions.

5. Discussion

5.1. LP Events

Over 6000 LP events are identified between March and September 2009. Five families of LP events are extracted using a cross-correlation technique. However, the similarity of these families (their stacks correlate with a correlation coefficient above 0.8) allows the 435 events in the families to be grouped into one large family. The subset of five families suggests minor changes in the source processes, the source locations or the structure through which the seismic waves are travelling. However, any changes in the source processes are likely to be very small as the moment tensor inversion gives very similar results for all of the events inverted. The source locations of the events also appear similar between families, but the resolution using the grid search method is not good enough to determine if the locations move small distances, which could be enough to produce small changes to the waveforms. It is therefore possible that the LP source is moving gradually, although it is not possible to determine in which direction(s). With regards to the structure of the volcano, the degree of water saturation could alter the seismic velocity of a medium, which would modify the waveforms of the LPs (Martini et al., 2009).

As well as changes within the family of events, there also appears to be a decrease in the percentage of LP events that correlate into a family after July 2009. This suggests that the LP events may be continually evolving and changing.

5.2. Source Locations

The results from the location method show that the LP events occur at shallow (<800m) depths, in good agreement with studies from other volcanoes (Almendros et al., 2001; Cusano et al., 2008; De

Barros et al., 2009; Kumagai et al., 2002; Lokmer et al., 2007; Nakano et al., 2003; Saccorotti et al., 2007). The locations have quite a large error (approximately ± 500 m) but the minimum residuals are located below the active Southwest and Central crater region. This is the region that contains the highly active hydrothermal and fumarolic systems with a magmatic intrusion beneath (Campion et al., 2012; Martini et al., 2010) and so it is likely that the LPs are related to these systems. As the depths are very shallow it is more likely that the LPs are related to the hydrothermal system, but a magmatic source cannot be ruled out as the magmatic body is believed to be at shallow depth (Campion et al., 2012; Martini et al., 2010).

5.3. Source Mechanisms

The best-fit mechanism for the LP events is a crack mechanism dipping shallowly to the southwest at approximately 10 to 20 °. A crack mechanism has been constrained at many volcanoes across the world as the likely mechanism for the generation of LP events (e.g. Chouet, 1996; Cusano et al., 2008; De Barros et al., 2011; Kumagai et al., 2005). The most widely-used model for the source mechanism of LP events attributes them to the resonance of a fluid-filled cavity (Chouet, 1988). As previously stated, the source locations are shallow and a highly active hydrothermal system exists in the Southwest and Central crater region where the events are located (Martini et al., 2010), so it is likely that the LPs are caused by hydrothermal processes rather than directly from the magmatic system. A resonating low angle (sub-horizontal) crack mechanism is believed to be the cause of LP events at Kilauea, Hawaii (Kumagai et al., 2005) and Kusatsu-Shirane volcano, Japan (Kumagai et al., 2002). In both these cases, the hydrothermal system is also interpreted to be the most likely source of LP events. The authors hypothesise that a crack containing hydrothermal fluid is pressurised by heating due to the presence of an underlying magma body. When the crack reaches a critical pressure level, there is a rapid discharge of the fluid, triggering the resonance of the crack. As a magma body is likely to be present beneath Turrialba volcano with the hydrothermal system overlying it (Campion et al., 2012; Martini et al., 2010), the same hypothesis could also apply here.

A problem for the LP events recorded at Turrialba volcano is that many of the waveforms at the summit of the volcano near to the source are pulse-like; not wholly consistent with the hypothesis that the events are generated by resonance. However, this could be explained by a high damping of the resonance, either due to a high viscosity fluid or low stiffness of the crack walls (Chouet, 1986). As the fluid is likely to be hydrothermal, it does not have a viscosity high enough to produce such significant damping. Low crack wall stiffness is more conceivable however, as the volcano is made up of layers of poorly consolidated tephra as well as more consolidated lavas and hydrothermally-altered rocks (Reagan et al., 2006). The less-stiff layers are more likely to contain the hydrothermal fluids as they are more likely to be permeable. Cracks may form parallel to the layering within these successive layers of tephras and lavas from previous eruptions as the layering is likely to create weaknesses within the structure, explaining the shallowly dipping orientations of the crack mechanisms. This could occur especially at the contacts between layers, as the layers are likely to be poorly bonded. As the volcanic centre has migrated over time to the southwest (Martini et al., 2010; Soto, 1988), the more recently formed summit craters have grown on the flanks of the previous craters: for example the Southwest crater on the southwest flank of the Central crater. The structures beneath the younger craters are therefore likely to have a layering sub-parallel to the flanks of the older craters. Beneath the Southwest crater, for example, the layers are likely to be dipping to the southwest due to the presence of the structure of the Central crater. As the craters are relatively close together, the depth to this underlying structure is likely to be shallow.

Another hypothesis arises due to a discontinuity that exists at ~ 900 m below the summit craters between the present cone stage (< 200 ka) and the previous edifice, Palaeo-Turrialba (250 ka) (Reagan et al., 2006). Such a discontinuity could influence the hydrothermal system since the older structure would be much more altered than the overlying younger material. This discontinuity is also likely to be dipping to the southwest below the Southwest crater. The consistent dip of the crack mechanism to the southwest can therefore be explained as the cracks generating LP events are likely exploiting the structure of the edifice.

The other possibility is that the hydrothermal fluid is "pulsing" through the crack, and this fits better with the pulse-like waveforms observed in the summit region. Similar conclusions were reached for LP events at Mt. Etna where crack mechanisms were found for events with comparably pulse-like waveforms (Lokmer et al., 2007). Again, the crack through which the fluid is "pulsing" may form parallel to the structural layering within the volcano, perhaps due to the hot rising hydrothermal fluid encountering an impermeable lava layer and so being forced to move laterally around it.

An alternative hypothesis to explain the pulse-like signals cannot be ruled out. For example, these events might be related to the deformation of the edifice (De Barros et al., 2011) in response to cycles of pressurisation/depressurisation associated to gas outputs. In this case LPs might be generated by crack opening/closing.

5.4. Robustness of the Solutions

The moment tensor inversion appears to be robust as it gives similar results in both mechanism and orientation, i.e. a crack mechanism dipping shallowly to the southwest, (1) for all five events that are inverted, (2) with single forces included or not, and (3) with constrained inversions. The solutions are also similar when the source locations are moved 500 m from the original location in all three directions (north-south, east-west and vertical), showing that a shallowly dipping crack mechanism is likely even if the source mechanism is mislocated. This means that even if the location obtained through the moment tensor inversion is not very precise, this method leads to accurately determined mechanisms. As shown by Lokmer et al. (2007) and Kumagai et al. (2010), joint inversion for location and mechanism can lead to spurious results. However, the network coverage, including stations very close to the hypocentre, allow here for a robust characterisation of the mechanism (Bean et al., 2008).

Another possible source of errors is the velocity model used when calculating the Green's functions, as there are no seismic velocity models available for Turrialba volcano. Ideally, further investigation into the seismic velocity structure at Turrialba volcano could be carried out to gain better constraints. However, this is not presently possible so a homogeneous velocity model is chosen. While this is not

likely to represent the real structure at Turrialba volcano, introducing more complex velocity structures without realistic constraints would likely generate further errors in the solution rather than improve it. The results presented here are therefore as accurate as possible at the current time. Even with a better velocity model, errors are still likely as volcanoes are highly heterogeneous structures, so simplifications are always required.

6. Conclusion

Results for the location and mechanism of LP events recorded at Turrialba volcano, Costa Rica in 2009 using full waveform moment tensor inversion have been presented. LP events at Turrialba volcano are generated by a crack mechanism dipping at a shallow angle towards the southwest, located at shallow depths between the active Southwest and Central craters. Using accepted models for the generation of LP events, the events are most likely to be generated in the hydrothermal system, either by resonance of a fluid-filled crack due to pressure fluctuations in the fluid or due to the fluid "pulsing" through the crack. The "pulsing" hypothesis seems more likely due to the pulse-like waveforms observed at the summit stations. The crack orientation is parallel to the likely orientation of layering of tephra and lava within the volcano, suggesting that the cracks form at weaknesses within the structure of the volcano edifice.

Acknowledgements

This work has been funded by Science Foundation Ireland (SFI), Contract No. 09/RFP/GEO2242. Field work was partially supported by the projects: "Estudio de la evolución geológica y petrológica del volcán Turrialba: implicaciones para la evolución volcánica de Costa Rica y prevención de riesgos volcánicos", N° 113-A9-509 and "Atenuación sísmica en el volcán Turrialba y su implicación para terrenos volcánicos y en la generación de grandes deslizamientos", N° 113-A9-508, financed by CONARE (National Council of Rectors from Costa Rica). We are grateful to Red Sismológica Nacional (RSN: UCR-ICE), particularly Carlos Redondo and Luis Fernando Brenes, for supporting the logistical work and the data acquisition. We are also grateful to the Cordillera Volcánica Central

Conservation Area staff for the facilities provided during the field work at Turrialba Volcano National Park.

References

Aki, K. and Richards, P.G., 2002. Quantitative seismology 2nd ed. University Science Books, Sausalito, California, 700 pp.

Almendros, J., Chouet, B. and Dawson, P., 2001. Spatial extent of a hydrothermal system at Kilauea Volcano, Hawaii, determined from array analyses of shallow long-period seismicity 2. Results. Journal of Geophysical Research, 106(B7): 13581-13597.

Barquero, R. and Rojas, W., 2011. Resumen de la actividad sísmica y volcánica en Costa Rica durante el año 2010. Revista Geológica de América Central, 44: 157-166.

Bean, C.J., Lokmer, I. and O'Brien, G.S., 2008. Influence of near-surface volcanic structure on long-period seismic signals and on moment tensor inversions: Simulated examples from Mount Etna. Journal of Geophysical Research, 113(B8).

Campion, R., Martinez-Cruz, M., Lecocq, T., Caudron, C., Pacheco, J., Pinardi, G., Hermans, C., Carn, S. and Bernard, A., 2012. Space- and ground-based measurements of sulphur dioxide emissions from Turrialba Volcano (Costa Rica). Bulletin of Volcanology: 1-14.

Chouet, B., 1986. Dynamics of a fluid-driven crack in three dimensions by the finite difference method. Journal of Geophysical Research, 91(B14): 13967-13992.

Chouet, B., 1988. Resonance of a fluid-driven crack: radiation properties and implications for the source of long-period events and harmonic tremor. Journal of Geophysical Research, 93(B5): 4375-4400.

Chouet, B., 1996. Long-period volcano seismicity: its source and use in eruption forecasting. Nature, 380: 309-316.

Chouet, B., 2003. Volcano seismology. Pure and Applied Geophysics, 160(3): 739-788.

Chouet, B., Dawson, P., Ohminato, T., Martini, M., Saccorotti, G., Giudicepietro, F., De Luca, G., Milana, G. and Scarpa, R., 2003. Source mechanisms of explosions at Stromboli Volcano, Italy, determined from moment-tensor inversions of very-long-period data. Journal of Geophysical Research, 108(B1).

Chouet, B.A. and Matoza, R.S., 2013. A multi-decadal view of seismic methods for detecting precursors of magma movement and eruption. Journal of Volcanology and Geothermal Research, 252: 108-175.

Cusano, P., Petrosino, S. and Saccorotti, G., 2008. Hydrothermal origin for sustained Long-Period (LP) activity at Campi Flegrei Volcanic Complex, Italy. Journal of Volcanology and Geothermal Research, 177(4): 1035-1044.

Davi, R., O'Brien, G.S., Lokmer, I., Bean, C.J., Lesage, P. and Mora, M.M., 2010. Moment tensor inversion of explosive long period events recorded on Arenal volcano, Costa Rica,

constrained by synthetic tests. Journal of Volcanology and Geothermal Research, 194(4): 189-200.

De Barros, L., Bean, C.J., Lokmer, I., Saccorotti, G., Zuccarello, L., O'Brien, G.S., Métaxian, J.-P. and Patanè, D., 2009. Source geometry from exceptionally high resolution long period event observations at Mt Etna during the 2008 eruption. Geophysical Research Letters, 36(24).

De Barros, L., Lokmer, I., Bean, C.J., O'Brien, G.S., Saccorotti, G., Métaxian, J.P., Zuccarello, L. and Patanè, D., 2011. Source mechanism of long-period events recorded by a high-density seismic network during the 2008 eruption on Mount Etna. Journal of Geophysical Research, 116(B1).

Ferrazzini, V. and Aki, K., 1987. Slow waves trapped in a fluid-filled infinite crack: implication for volcanic tremor. Journal of Geophysical Research, 92(B9): 9215-9223.

Gilbert, J.S. and Lane, S.J., 2008. The consequences of fluid motion in volcanic conduits. Geological Society, London, Special Publications, 307(1): 1-10.

Jolly, A.D., Sherburn, S., Jousset, P. and Kilgour, G., 2010. Eruption source processes derived from seismic and acoustic observations of the 25 September 2007 Ruapehu eruption—North Island, New Zealand. Journal of Volcanology and Geothermal Research, 191(1–2): 33-45.

Jousset, P., Neuberg, J. and Jolly, A., 2004. Modelling low-frequency volcanic earthquakes in a viscoelastic medium with topography. Geophysical Journal International, 159(2): 776-802.

Kumagai, H., Chouet, B. and Nakano, M., 2002. Waveform inversion of oscillatory signatures in long-period events beneath volcanoes. Journal of Geophysical Research, 107(B11).

Kumagai, H., Chouet, B.A. and Dawson, P.B., 2005. Source process of a long-period event at Kilauea volcano, Hawaii. Geophysical Journal International, 161(1): 243-254.

Kumagai, H., Nakano, M., Maeda, T., Yepes, H., Palacios, P., Ruiz, M., Arrais, S., Vaca, M., Molina, I. and Yamashima, T., 2010. Broadband seismic monitoring of active volcanoes using deterministic and stochastic approaches. Journal of Geophysical Research, 115(B8): B08303.

Lokmer, I., Bean, C.J., Saccorotti, G. and Patanè, D., 2007. Moment-tensor inversion of LP events recorded on Etna in 2004 using constraints obtained from wave simulation tests. Geophysical Research Letters, 34(22).

Martini, F., Bean, C.J., Saccorotti, G., Viveiros, F. and Wallenstein, N., 2009. Seasonal cycles of seismic velocity variations detected using coda wave interferometry at Fogo volcano, São Miguel, Azores, during 2003–2004. Journal of Volcanology and Geothermal Research, 181(3–4): 231-246.

Martini, F., Tassi, F., Vaselli, O., Del Potro, R., Martinez, M., del Laat, R.V. and Fernandez, E., 2010. Geophysical, geochemical and geodetical signals of reawakening at Turrialba volcano (Costa Rica) after almost 150 years of quiescence. Journal of Volcanology and Geothermal Research, 198(3-4): 416-432.

Montoya, C.L., 2009. Informe del estudio geofisico en un perfil en la cima del volcan Turrialba, Technical Report.

Nakano, M. and Kumagai, H., 2005. Response of a hydrothermal system to magmatic heat inferred from temporal variations in the complex frequencies of long-period events at Kusatsu-Shirane Volcano, Japan. Journal of Volcanology and Geothermal Research, 147(3-4): 233-244.

Nakano, M., Kumagai, H. and Chouet, B.A., 2003. Source mechanism of long-period events at Kusatsu–Shirane Volcano, Japan, inferred from waveform inversion of the effective excitation functions. Journal of Volcanology and Geothermal Research, 122(3-4): 149-164.

Neuberg, J.W., Tuffen, H., Collier, L., Green, D., Powell, T. and Dingwell, D., 2006. The trigger mechanism of low-frequency earthquakes on Montserrat. Journal of Volcanology and Geothermal Research, 153(1-2): 37-50.

O'Brien, G.S. and Bean, C., 2004. A 3D discrete numerical elastic lattice method for seismic wave propagation in heterogeneous media with topography. Geophysical Research Letters, 31(14).

Ohminato, T., Chouet, B.A., Dawson, P. and Kedar, S., 1998. Waveform inversion of very long period impulsive signals associated with magmatic injection beneath Kilauea Volcano, Hawaii. Journal of Geophysical Research, 103(B10): 23839-23862.

Reagan, M.K., Duarte, E., Soto, G.J. and Fernandez, E., 2006. The eruptive history of Turrialba volcano, Costa Rica, and potential hazards from future eruptions. Geological Society of America Special Paper(Volcanic hazards in Central America): 235-257.

Ripperger, J., Igel, H. and Wasserman, J., 2003. Seismic wave simulation in the presence of real volcano topography. Journal of Volcanology and Geothermal Research, 128(1-3): 31-44.

Rust, A.C., Balmforth, N.J. and Mandre, S., 2008. The feasibility of generating low-frequency volcano seismicity by flow through a deformable channel. Geological Society, London, Special Publications, 307(1): 45-56.

Saccorotti, G., Lokmer, I., Bean, C., Digrazia, G. and Patane, D., 2007. Analysis of sustained long-period activity at Etna Volcano, Italy. Journal of Volcanology and Geothermal Research, 160(3-4): 340-354.

Soto, G.J., 1988. Estructuras volcano-tectonicas del volcan Turrialba, Costa Rica, America Central, Actas Quinto Congreso Geologico Chileno, Santiago, pp. 163-175.

Soto, G.J. and Mora, M., 2013. Actividad del volcán Turrialba (2007-2011) y perspectivas de amenaza volcánica, Costa Rica en el tercer milenio: desafíos y propuestas para la reducción de vulnerabilidad ante los desastres, Preventec. UCR, pp. 287-310.

Soto, G.J., Mora, R., Mora, M.M., Barquero, R., Taylor, W., Vargas, A., Alvarado, G.E., Ramírez, C., González, G., Mora, R., Paniagua, C. and Fernández, J.F., 2010. Turrialba volcano's threat to the cities of the Central Valley of Costa Rica, Cities on Volcanoes 6, Puerto de la Cruz, Tenerife, pp. 138.

Takei, Y. and Kumazawa, M., 1994. Why have the single force and torque been excluded from seismic source models? Geophysical Journal International, 118(1): 20-30.

Tassi, F., Vaselli, O., Barboza, V., Fernandez, E. and Duarte, E., 2004. Fluid geochemistry and seismic activity in the period 1998-2002 at Turrialba Volcano (Costa Rica). Annals of Geophysics, 47(4): 1501-1511.

Varley, N., Arámbula-Mendoza, R., Reyes-Dávila, G., Sanderson, R. and Stevenson, J., 2010. Generation of Vulcanian activity and long-period seismicity at Volcán de Colima, Mexico. Journal of Volcanology and Geothermal Research, 198(1-2): 45-56.

Vasco, D.W., 1989. Deriving source-time functions using principal component analysis. Bulletin of the Seismological Society of America, 79(3): 711-730.

Vaselli, O., Tassi, F., Duarte, E., Fernandez, E., Poreda, R. and Huertas, A., 2010. Evolution of fluid geochemistry at the Turrialba volcano (Costa Rica) from 1998 to 2008. Bulletin of Volcanology, 72(4): 397-410.

Vavryčuk, V., 2001. Inversion for parameters of tensile earthquakes. Journal of Geophysical Research, 106(B8): 16339-16355.

Figure Captions

Figure 1a - Map of the location of Turrialba volcano in Costa Rica.

Figure 1b - Map of the 2009 broadband seismic network at Turrialba volcano. Triangles show seismic stations and contours are in km a.s.l..

Figure 2 – Seismogram recorded on the vertical component at station CIMA and the corresponding spectrogram. The event at 40s is classified as an LP event, with most of its energy below 5 Hz, and is picked up using the modified STA/LTA technique. The event at 70s is not picked up due to the large proportion of high frequency energy.

Figure 3a - LP event used in the full-waveform moment tensor inversion, shown normalised for the vertical component at all stations, and ordered with the distance from the active Southwest Crater. Note the pulse-like waveform on the summit stations, which becomes oscillating for stations further from the summit.

Figure 3b - LP event used for the full-waveform moment tensor inversion and its frequency spectrum, recorded in 2009 on the vertical component at station CIMA (also shown filtered between 0.3-1.3Hz in red). This is the event used in the inversion example in figures 6 to 8.

Figure 4a - Waveform stacks from the original five families of LP events obtained using a cross-correlation technique, recorded in 2009 on the vertical component at station CIMA, filtered between 0.3 to 1.3 Hz. Note that the families are very similar. Numbers on the right give the number of events in each family.

Figure 4b – Waveform stack for the family of events from 2009, recorded on the vertical component at station CIMA. All events that correlated into a family are combined into this family of 435 events.

Figure 5 – Temporal distribution of LP events showing the number of LP events per day for the duration of the experiment (red) and the temporal distribution of LP events in the family (black). Note that the station used to identify families, CIMA, was not operational between 10th and 22nd July, hence the gap in the data.

Figure 6 - Location of the LP event from figure 3 calculated using moment tensor inversion for a 3D grid of possible source locations below the volcano. The gridpoint with the lowest residual (blue) between real and synthetic data gives the most likely source location. The vertical slices are taken through the point with the minimum residual. The horizontal slice on the right is taken at 2660m a.s.l.. Approximate locations of the Southwest (SW) and Central (C) craters are shown in white and the black star shows the point which has the minimum residual. The location is between the Southwest and Central craters at shallow (< 800 m) depth, although the depth is poorly constrained.

Figure 7 - Moment tensor solutions and their eigenvectors (i) including single forces and (ii) without single forces for the LP event shown in figure 3, using the optimum source location shown in figure 6. Eigenvectors are sampled every 0.002s when the amplitude of one of the components is greater than 99% of the maximum amplitude. The eigenvector ratios and the proportion of isotropic (Iso), CLVD and double couple (DC) components are labelled. Both solutions show that the most likely source mechanism for the LP event is a crack mechanism dipping at low angles to the southwest parallel to the two smaller eigenvectors.

Figure 8 – Normalised waveform fits from the moment tensor inversion for each component (from left to right E, N, Z) at each station for (a) moment tensor components only, and (b) when single forces are included in the inversion. The real data is shown in blue and the reconstructed data in red.

Table Captions

Table 1 - Results from the principle component analyses of the optimum moment tensor solutions for five events excluding single forces, using the methods of Vasco (1989) and Vavryčuk (2001).

Table 2 Results from the principle component analyses of the optimum moment tensor solutions for five events including single forces, using the methods of Vasco (1989) and Vavryčuk (2001).

(a)

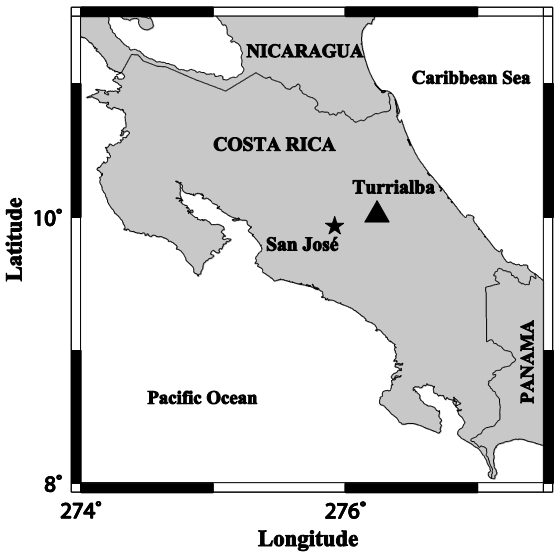
NICARAGUA
Caribbean Sea
COSTA RICA
Turrialba
San José
PANAMA
Pacific Ocean
Latitude
10°
8°
274°
276°
Longitude

(b)

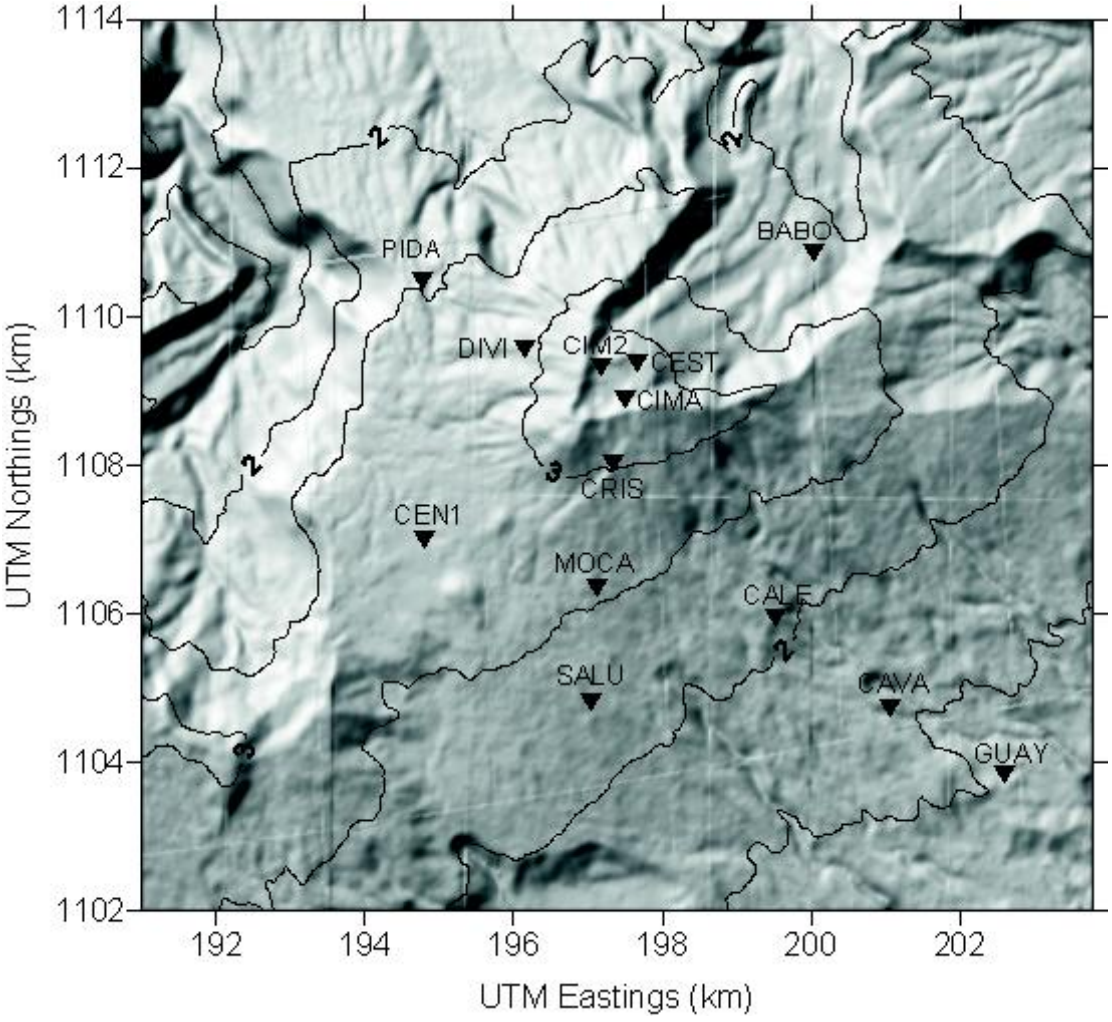
PIDA
BABO
DIVI
CIM2
CEST
CIMA
CRIS
CEN1
MOCA
CALE
SALU
CAVA
GUAY
UTM Northings (km)
1114
1112
1110
1108
1106
1104
1102
192
194
196
198
200
202
UTM Eastings (km)

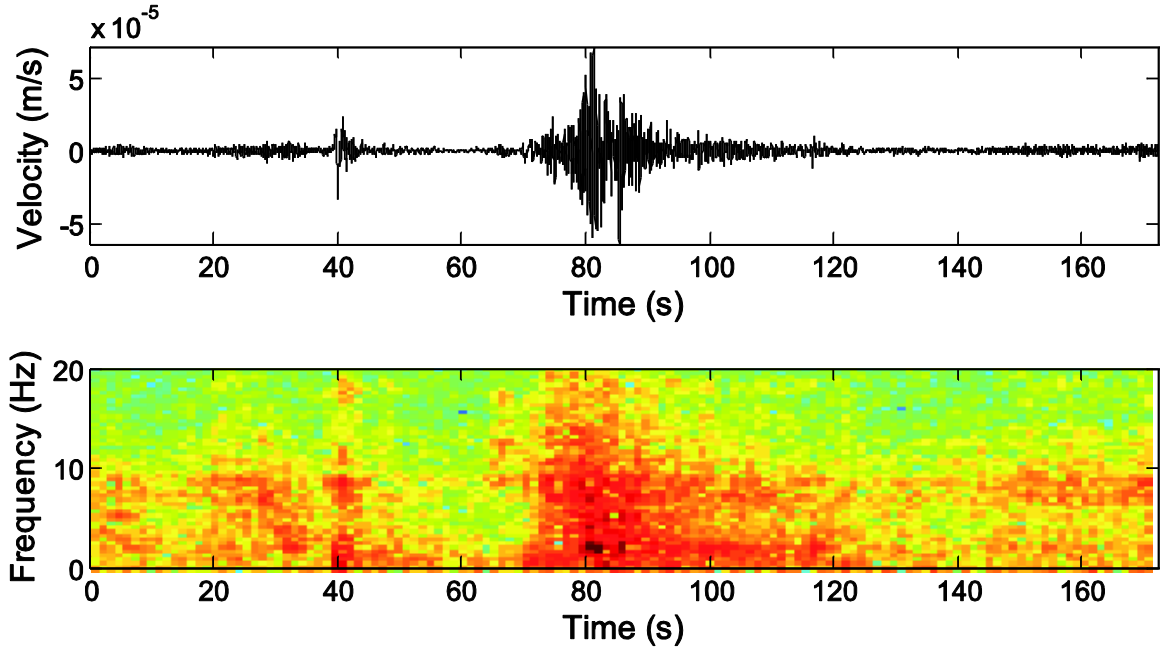
x 10^-5
Velocity (m/s)
5
0
-5
0
20
40
60
80
100
120
140
160
Time (s)
Frequency (Hz)
20
10
0
0
20
40
60
80
100
120
140
160
Time (s)

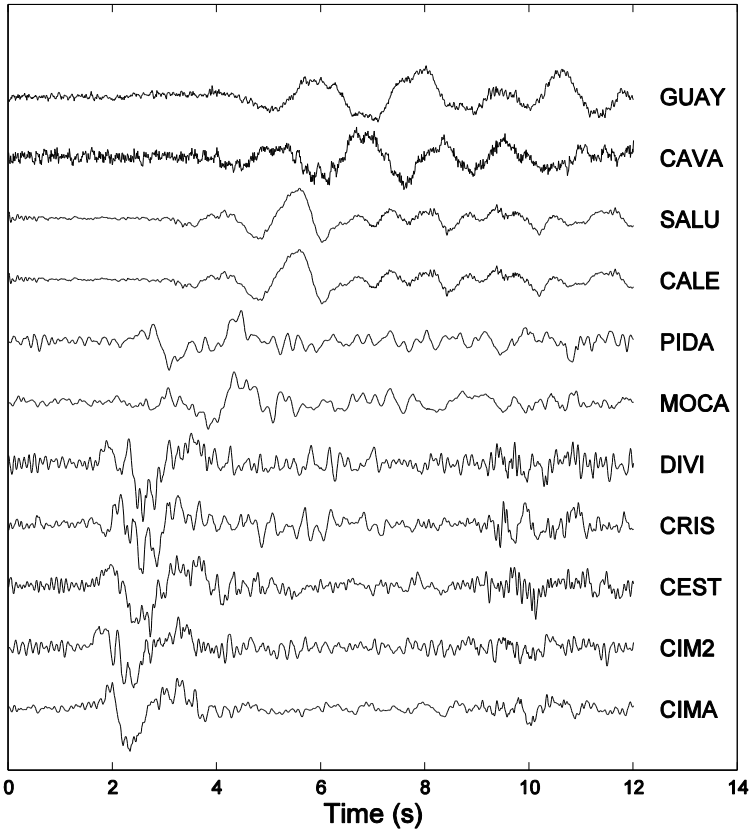
GUAY
CAVA
SALU
CALE
PIDA
MOCA
DIVI
CRIS
CEST
CIM2
CIMA
0
2
4
6
8
10
12
14
Time (s)

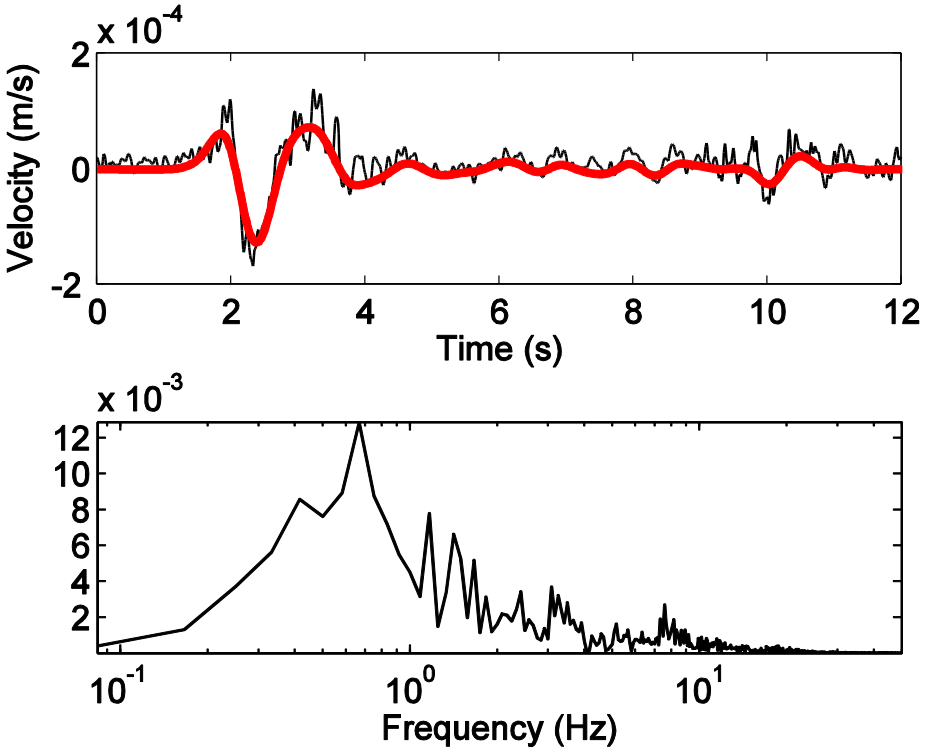
x 10-4
2
0
-2
Velocity (m/s)
0
2
4
6
8
10
12
Time (s)
x 10-3
12
10
8
6
4
2
10-1
100
101
Frequency (Hz)

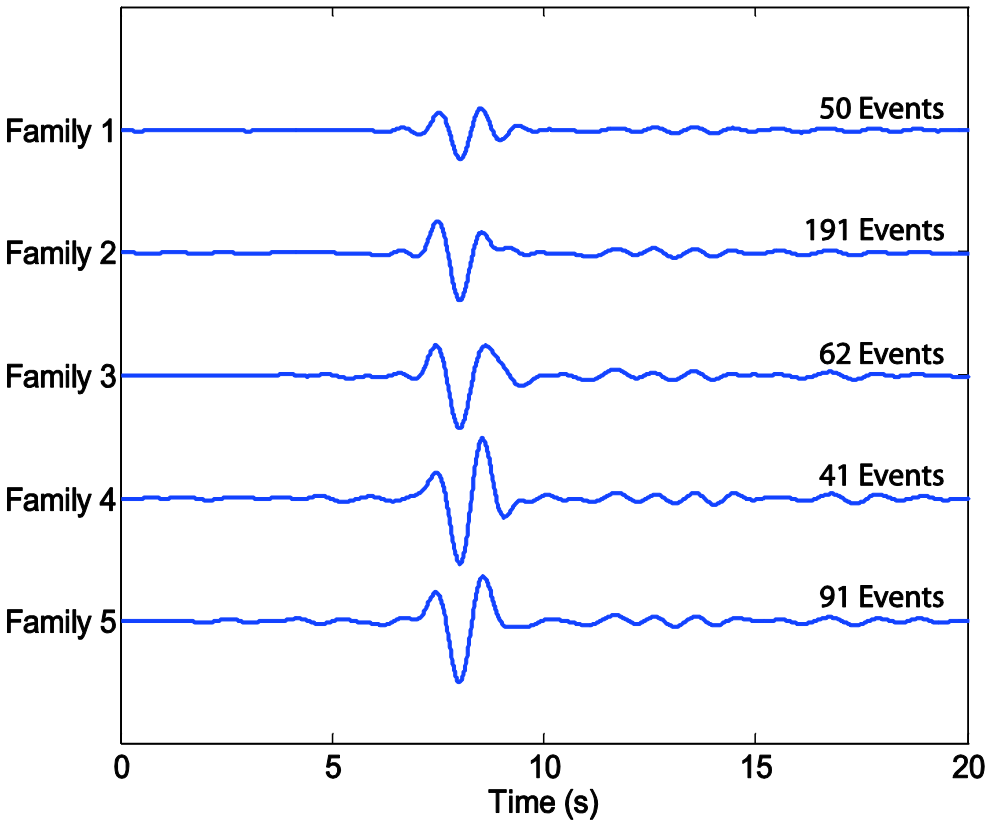
Family 1
50 Events
Family 2
191 Events
Family 3
62 Events
Family 4
41 Events
Family 5
91 Events
0
5
10
15
20
Time (s)

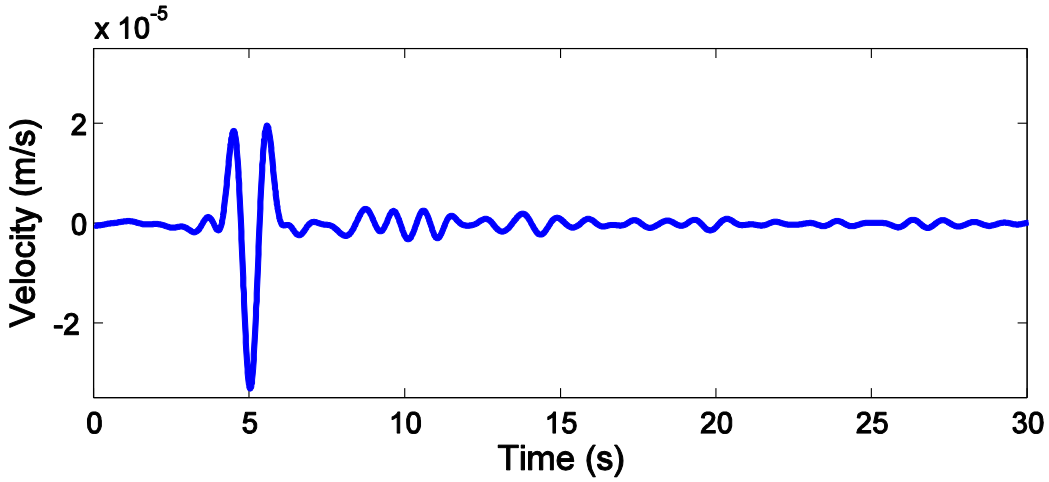
x 10-5
Velocity (m/s)
2
0
-2
0
5
10
15
20
25
30
Time (s)

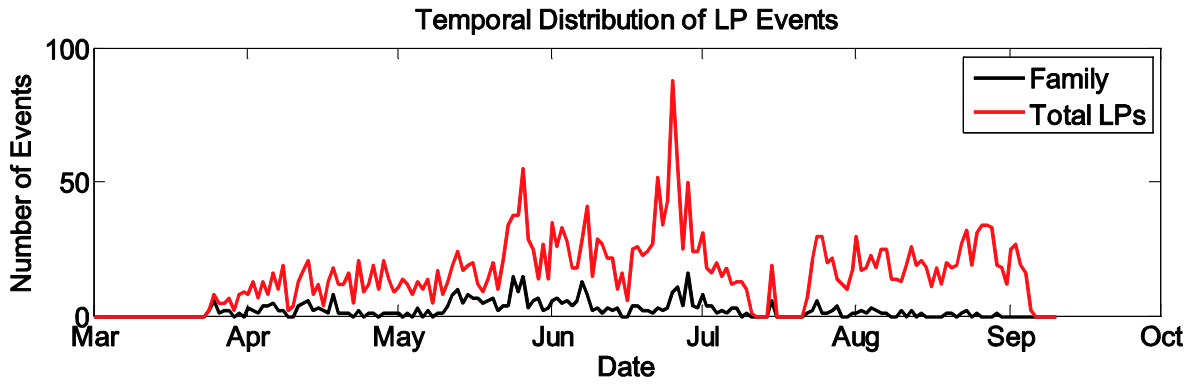
Temporal Distribution of LP Events
Number of Events
100
50
0
Mar
Apr
May
Jun
Jul
Aug
Sep
Oct
Date
Family
Total LPs

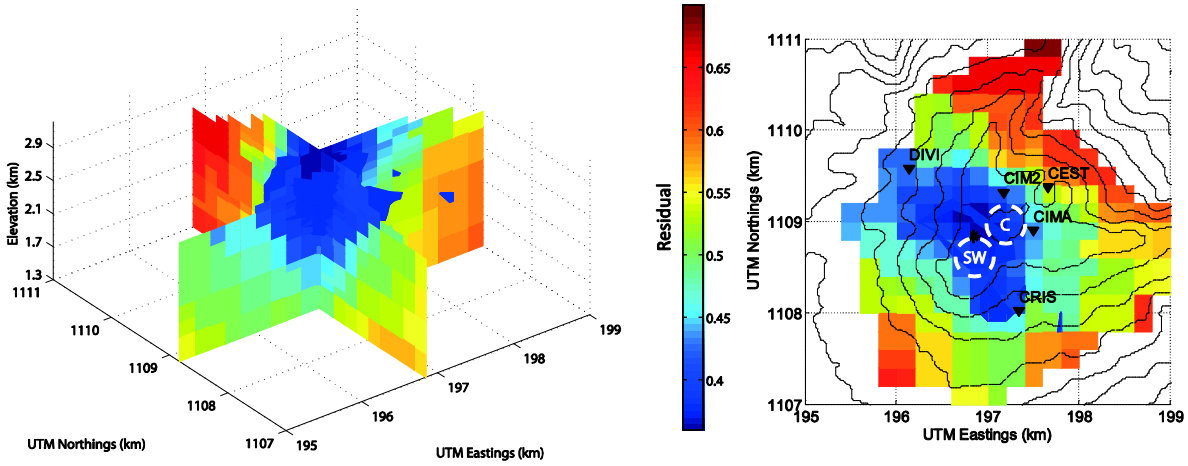
Elevation (km)
2.9
2.5
2.1
1.7
1.3
1111
1110
1109
1108
1107
UTM Northings (km)
195
196
197
198
199
UTM Eastings (km)
Residual
0.65
0.6
0.55
0.5
0.45
0.4
UTM Northings (km)
DIVI
CIM2
CEST
CIMA
C
SW
CRIS
UTM Eastings (km)

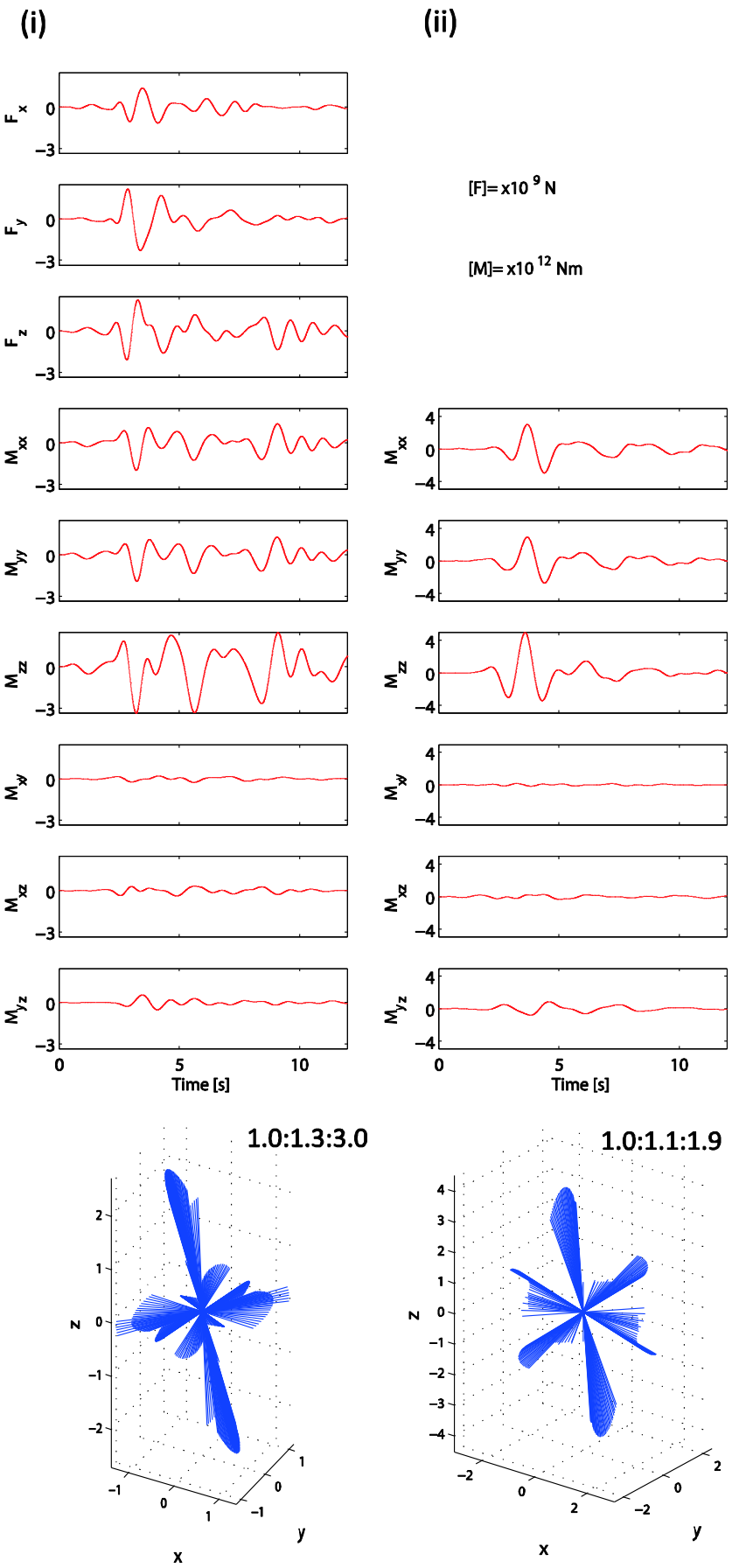
(i)
(ii)
[F]= x10 9 N
[M]= x10 12 Nm
F x
F y
F z
M xx
M yy
M zz
M xy
M xz
M yz
Time [s]
1.0:1.3:3.0
1.0:1.1:1.9
x
y
z

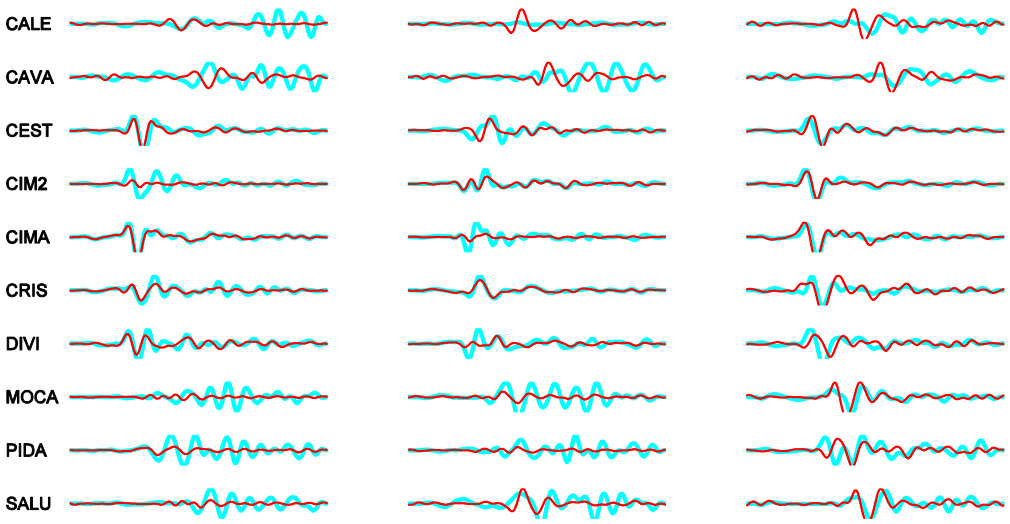
CALE
CAVA
CEST
CIM2
CIMA
CRIS
DIVI
MOCA
PIDA
SALU

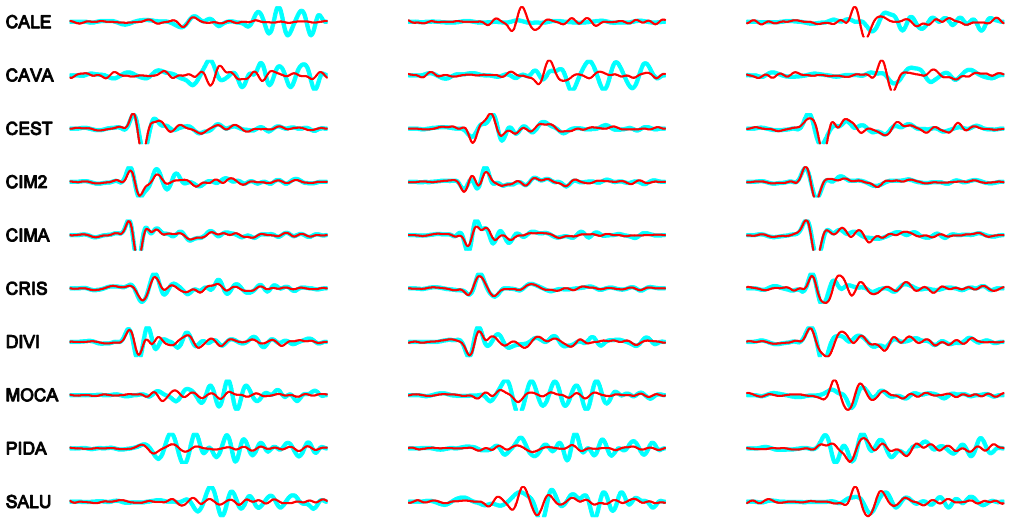
CALE
CAVA
CEST
CIM2
CIMA
CRIS
DIVI
MOCA
PIDA
SALU